Cosmology:

The Sunyaev-Zeldovich effect and large-scale structure of the Universe from the perspective of the CMB

Steven T. Myers

University of Bologna

and

the National Radio Astronomy Observatory – Socorro, NM

The SZE

- The Sunyaev-Zeldovich Effect
  - Compton upscattering of CMB photons by keV electrons
  - decrement in I below CMB thermal peak (increment above)
  - negative extended sources (absorption against 3K CMB)
  - massive clusters mK, but shallow profile $\theta^{-1} \rightarrow$ -exp(-v)

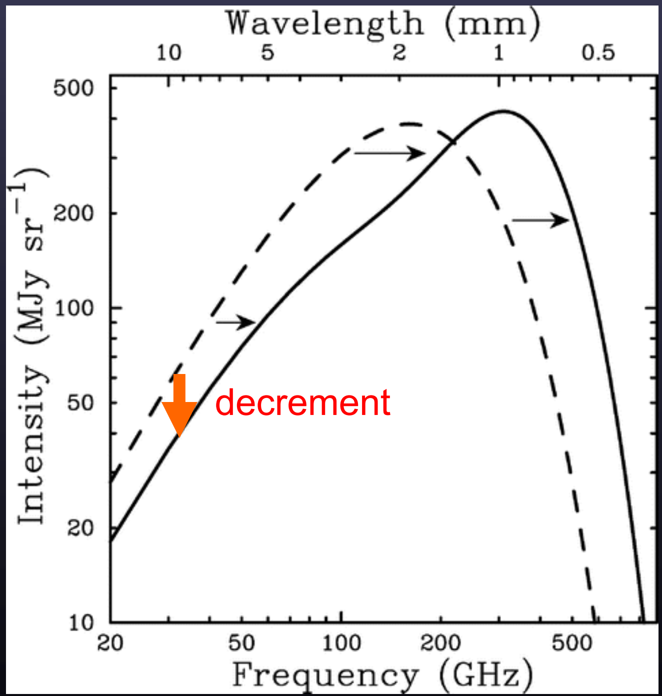

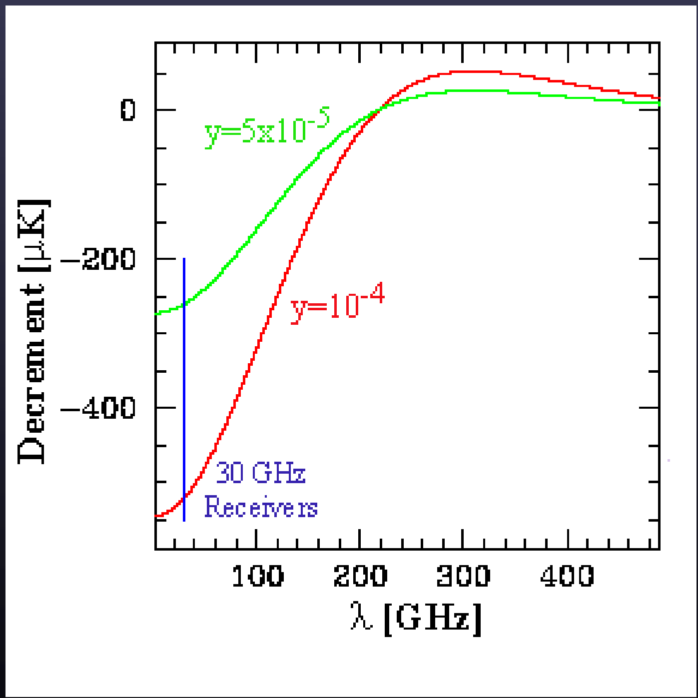

SZE vs. X-rays

- gas density profiles: $$n_e(r) = n_{e0}\left(1+\frac{r^2}{r_0^2}\right)^{-3\beta/2}$$
- X-ray surface brightness: $$b_X(E) = \frac{1}{4\pi(1+z)^3}\int n_e^2(r)\Lambda(E,T_e)\,dl$$
- SZE surface brightness: $$\Delta I_{\rm SZE} \propto T_e \int n_e\,dl$$
- <u>exploit different dependence on parameters:</u>
- use X-ray: $$b_X \propto n_{e0}^2\theta_0 D_A\left(1+\frac{\theta^2}{\theta_0^2}\right)^{-3\beta+1/2}$$ $\rightarrow$ $D_A \sim h^{-1}$ $n_{e0} \sim h^{1/2}$
- plug into SZE: $$\Delta I_{\rm SZE} \propto T_e n_{e0}\theta_0 D_A\left(1+\frac{\theta^2}{\theta_0^2}\right)^{-\frac{3}{2}\beta+\frac{1}{2}}$$ $\rightarrow$ $\Delta I_{SZE} \sim h^{-1/2}$

SZ visibilities

- Use standard interferometer equation with SZ profile:

$$V(u,v) = I_0 \int_{-\infty}^{\infty} \int_{-\infty}^{\infty} B(\theta) \left(1 + \frac{\theta^2}{\theta_0^2}\right)^{-\frac{3}{2}\beta+\frac{1}{2}} e^{2\pi i(ux+vy)}\, dx\, dy$$

- Spherical symmetry – integrate over azimuthal angle

$$V(u,v) = \int_0^{\infty} d\theta B(\theta) \frac{\theta}{\theta_0} \left(1 + \frac{\theta^2}{\theta_0^2}\right)^{-\frac{3\beta}{2}+\frac{1}{2}} J_0(2\pi\theta u)$$

- For $\beta = 2/3$ SZE $\Delta I \sim \theta^{-1} \rightarrow V \sim -\exp(-v)$
  - visibilities dominated by shortest baselines!
- Xray $\Delta I \sim \theta^{-3}$
  - SZ profile more extended than X-rays

Example: CBI visibilities

- CBI:

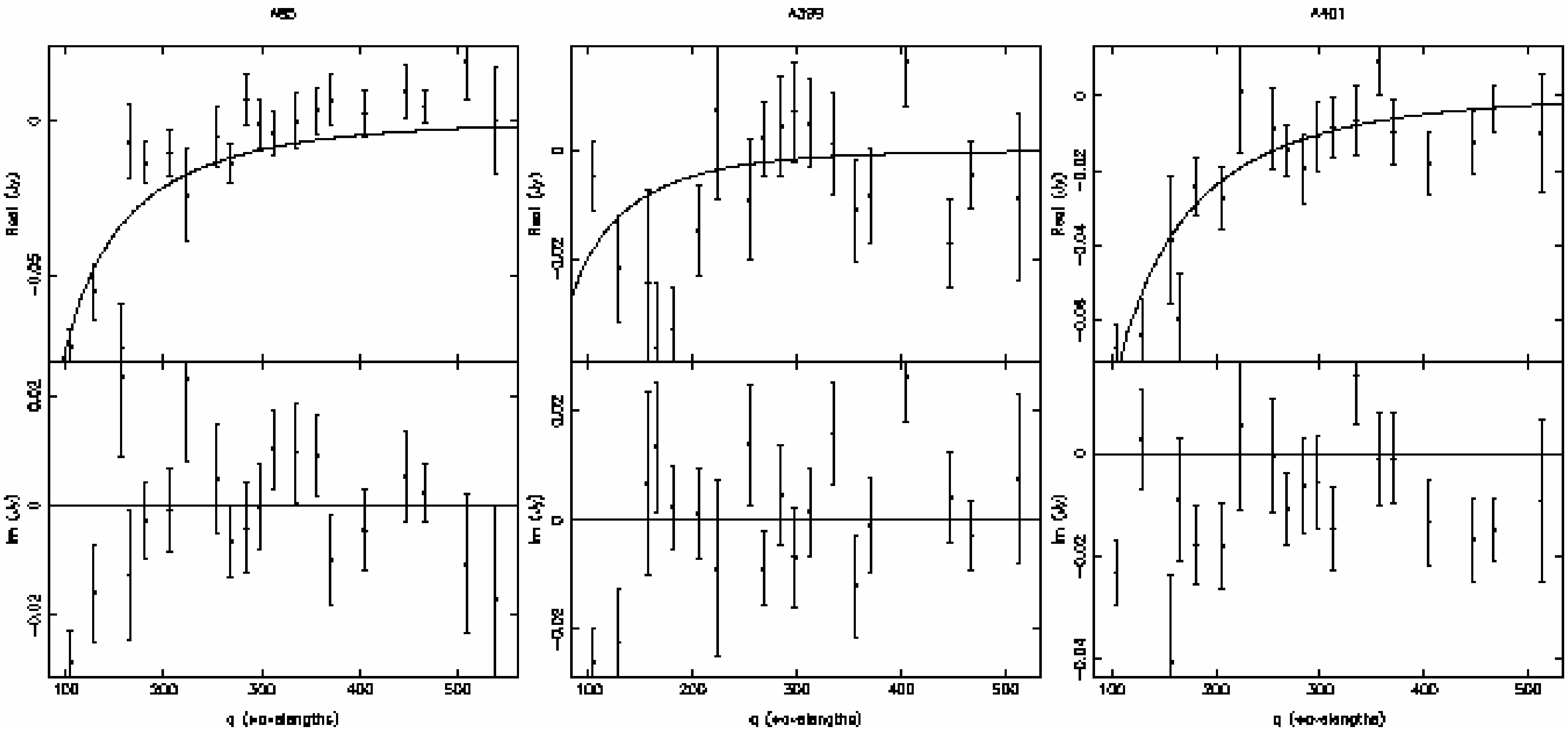

BIMA Observations

9 Telescopes in Compact Array

28.5 GHz Observing Frequency

6.6’ FWHM

~150 μJy/beam RMS (u-v < 1.1 kλ)

15 μK for 2’ Synthesized Beam

CL 0016+16, z = 0.55 (Carlstrom et al.)

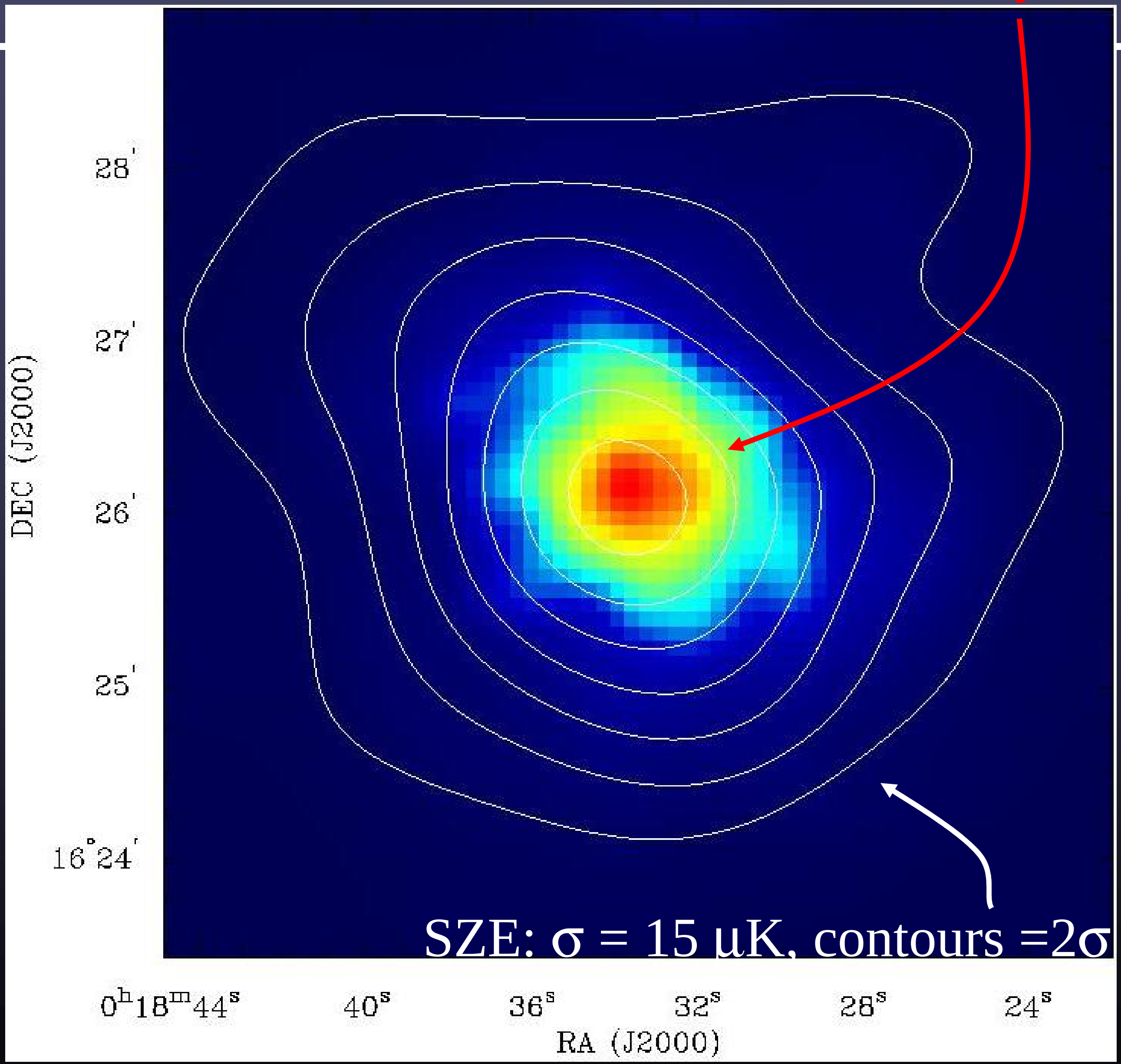

Sample from 60 OVRO/BIMA imaged clusters, $0.07 < z < 1.03$

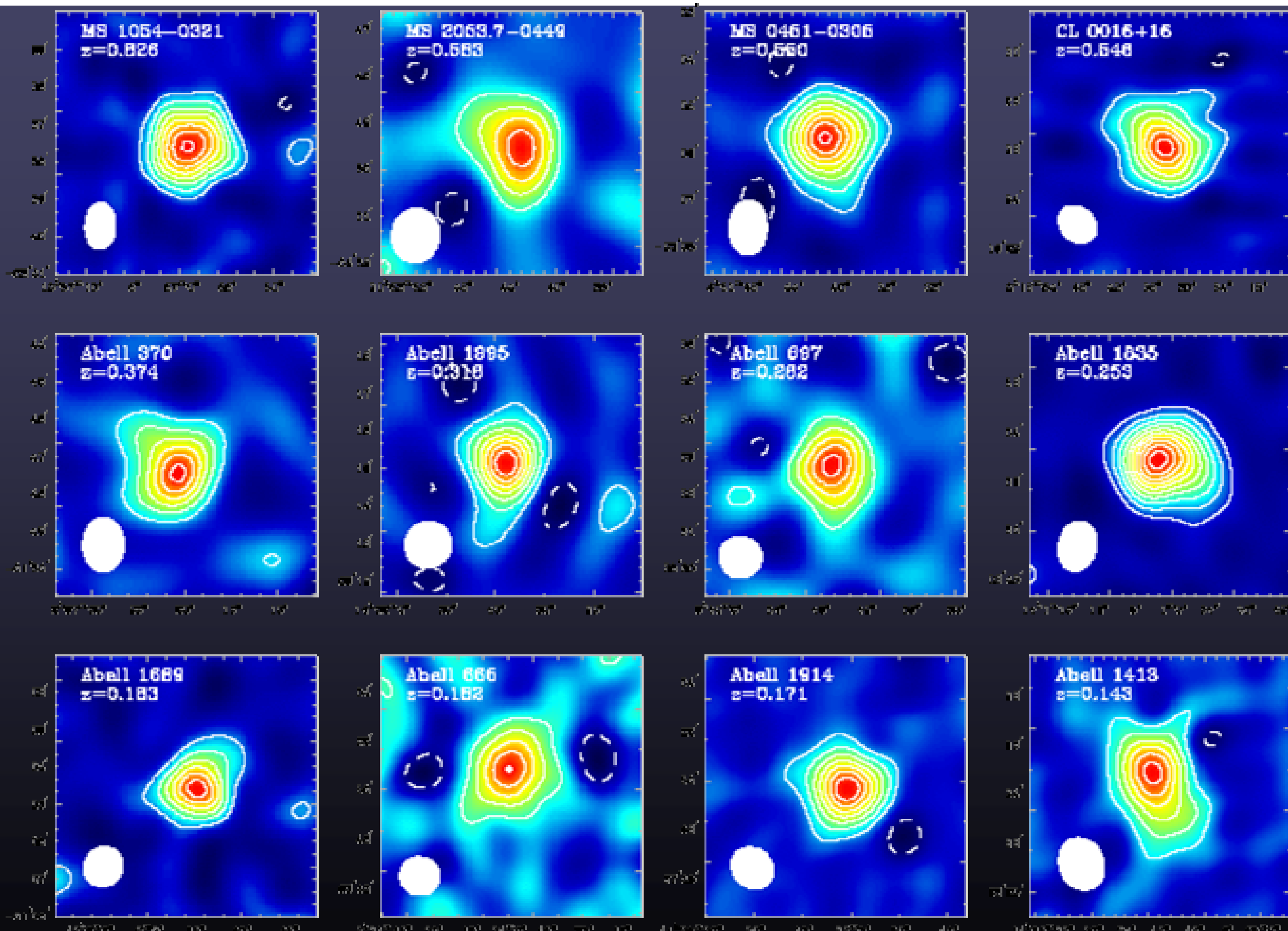

CBI

- 13 90-cm Cassegrain antennas
  - 78 baselines
- 6-meter platform
  - Baselines 1m – 5.51m
- 10 1 GHz channels 26-36 GHz
  - HEMT amplifiers (NRAO)
  - Cryogenic 6K, Tsys 20 K
- Single polarization (R or L)
  - Polarizers from U. Chicago
- Analog correlators
  - 780 complex correlators
- Field-of-view 44 arcmin
  - Image noise 4 mJy/bm 900s
- Resolution 4.5 – 10 arcmin

SZE CBI visibility function

- Xray: θ^{-3} ($\beta \sim 2/3$)
- SZE: $\theta^{-1} \rightarrow$ -exp(-v)
- dominated by shortest baselines

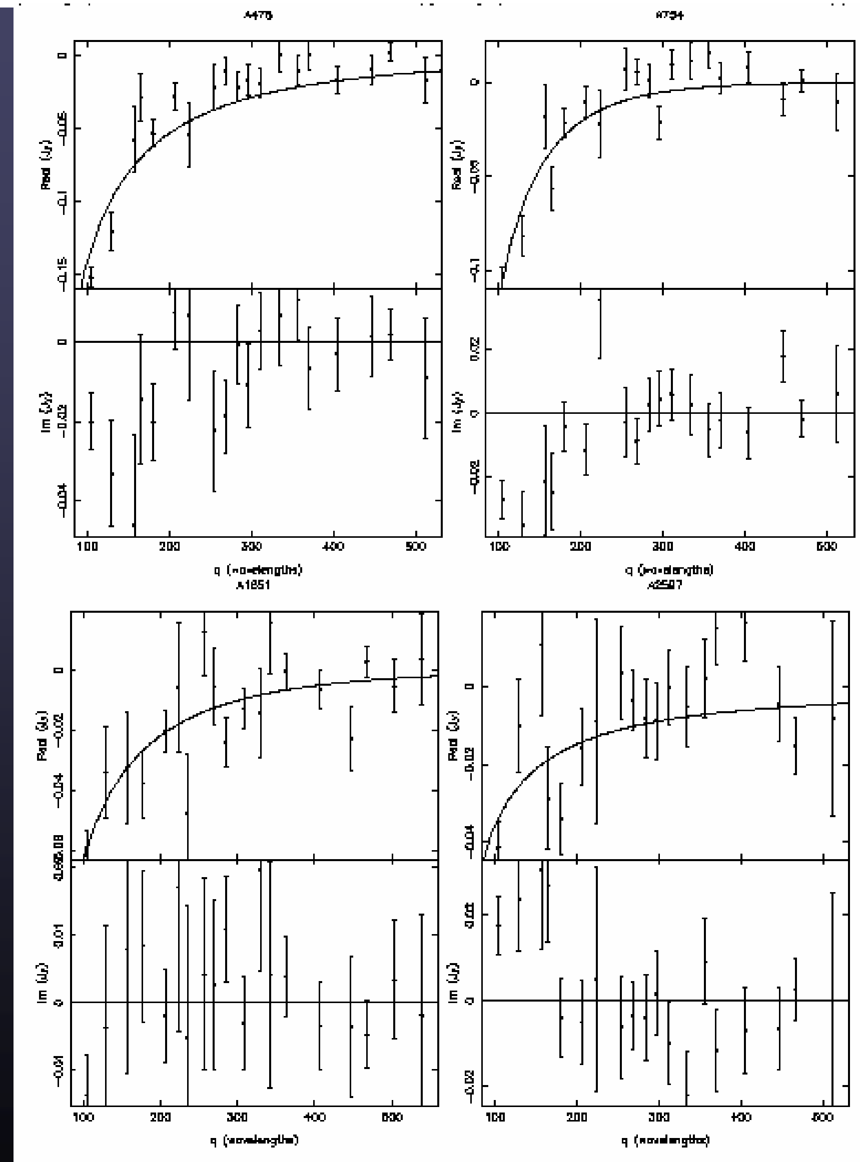

A85

Forman et al. astro-ph/0301476

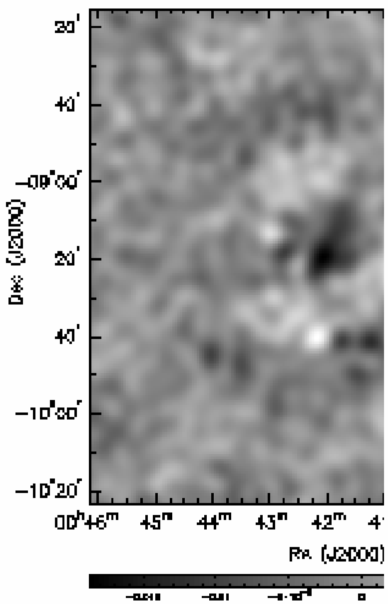

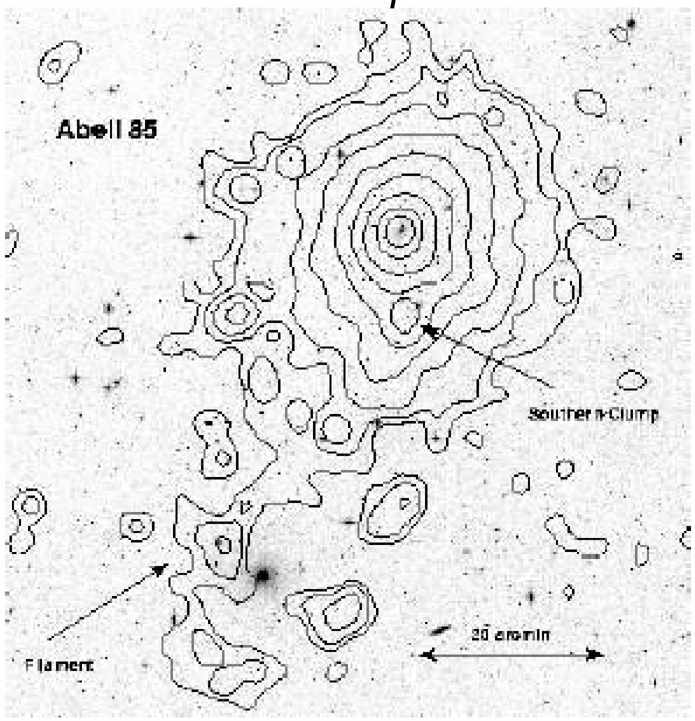

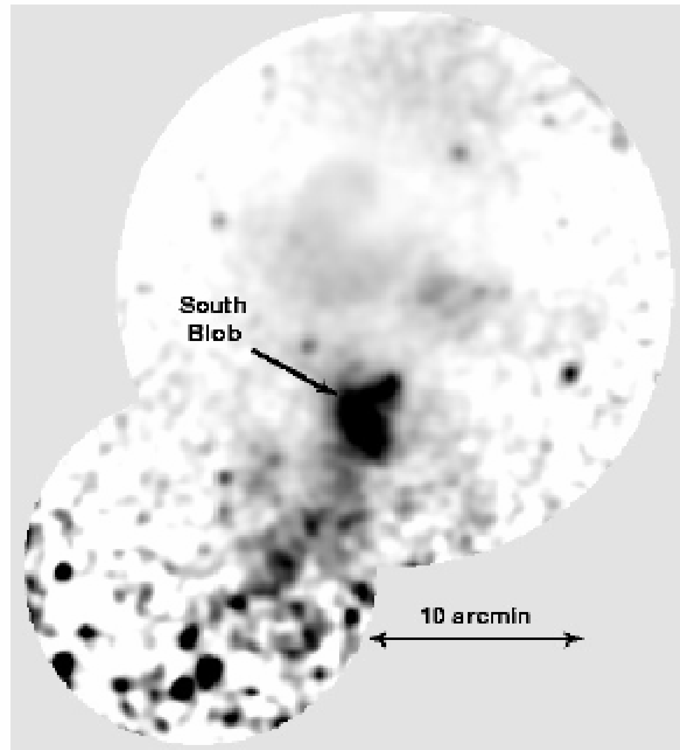

(left) Raw CBI Ima

Figure 1. ROSAT and XMM-Newton observations of A85 (**a**) ROSAT PSPC iso-intensity contours (0.4-2.0 keV) are shown superposed on an optical image (adapted from Durret et al. 1998). A filamentary structure extends to the southeast. (**b**) The XMM-Newton MOS image shows the inner portion of the filament extending southeast from the South Blob (Southern Clump) (Durret et al. 2003).

- A85 – cl
  activity,

A399

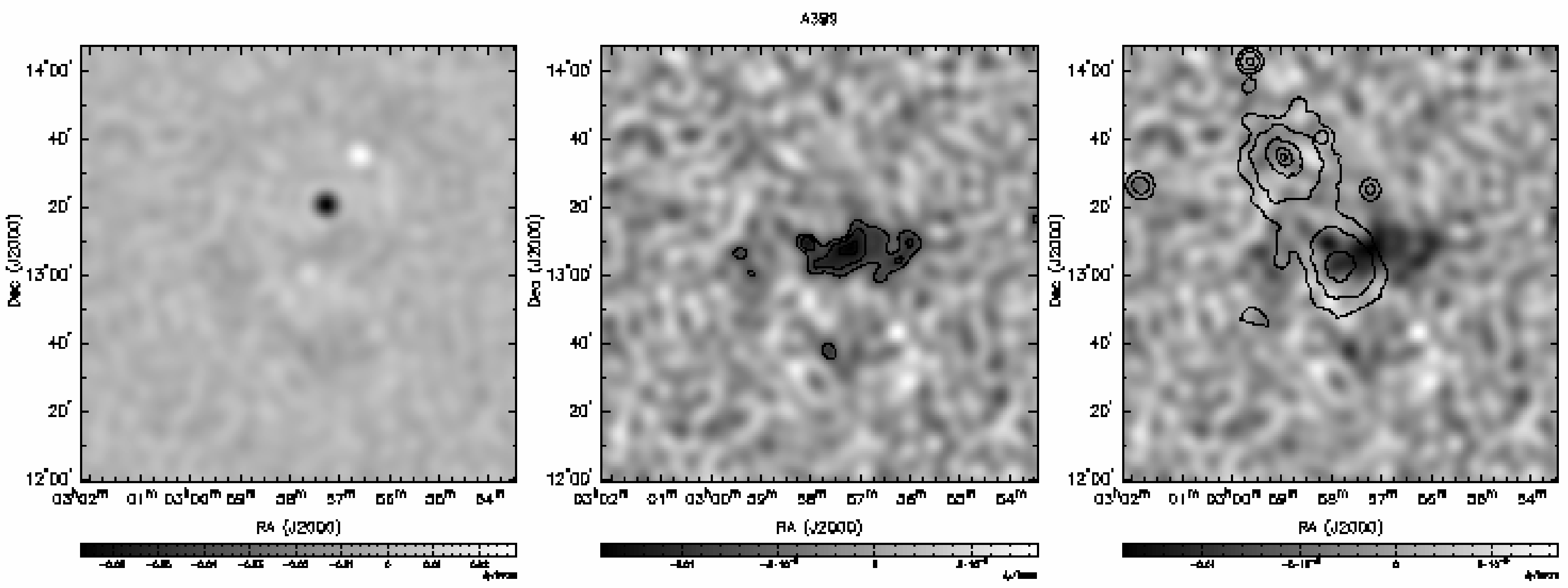

(left) Raw CBI Image (center) CLEAN source-sub CBI Image (right) CBI w/ROSAT

- A399 – pair with A401

A401

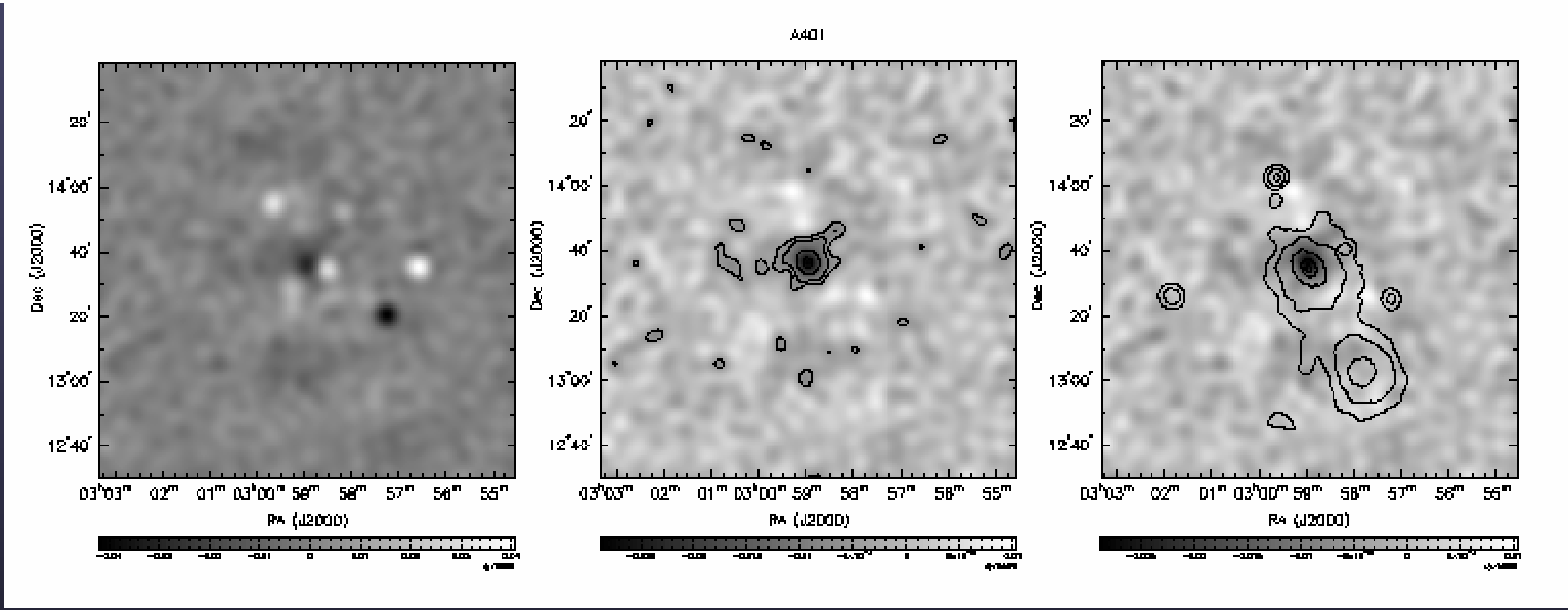

(left) Raw CBI Image (center) CLEAN source-sub CBI Image (right) CBI w/ROSAT

- A401 – pair with A399, likely interacting now or in past, cooling flow disrupted?

A478

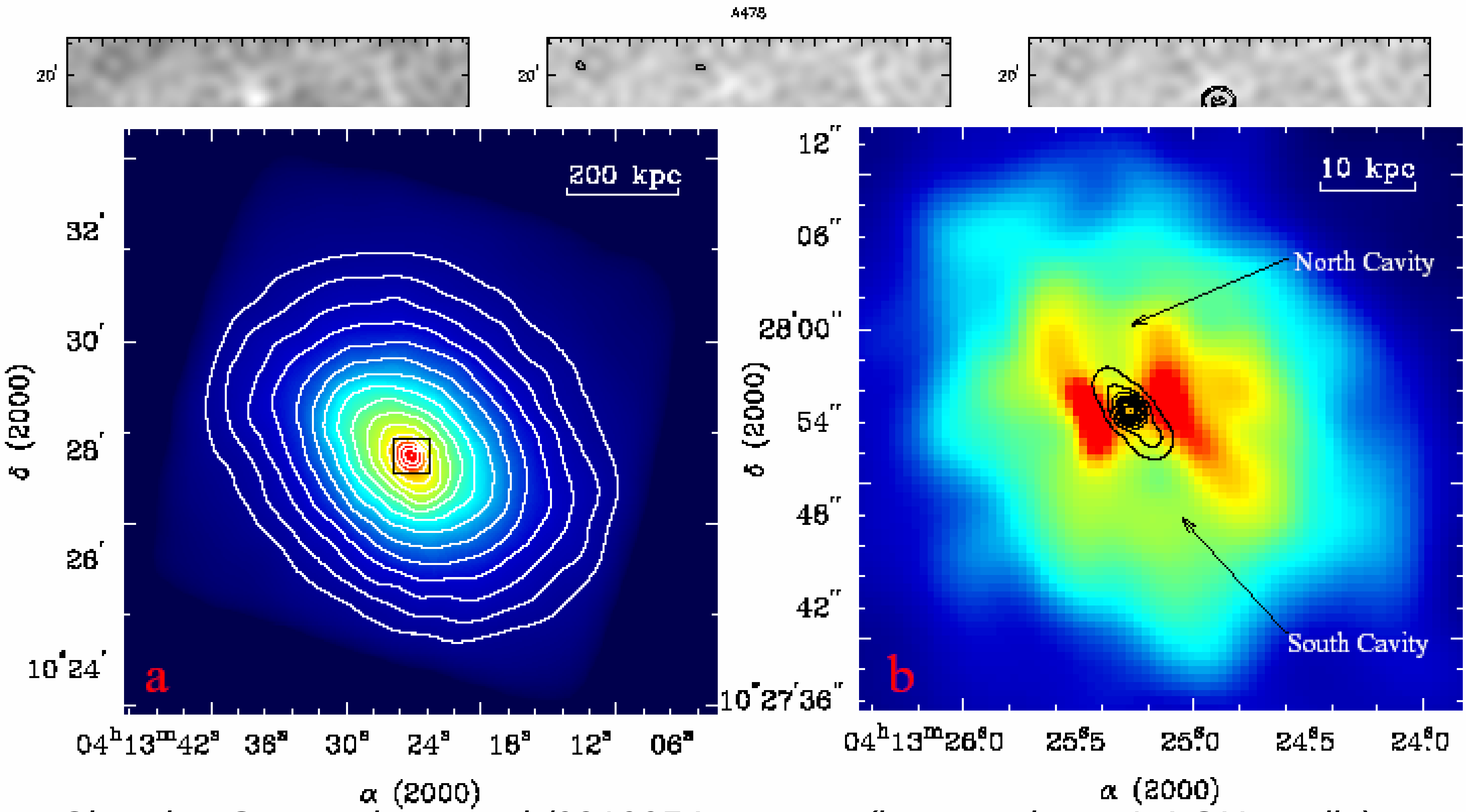

Chandra: Sun et al. astro-ph/0210054

(inner region + 1.4 GHz radio)

A754

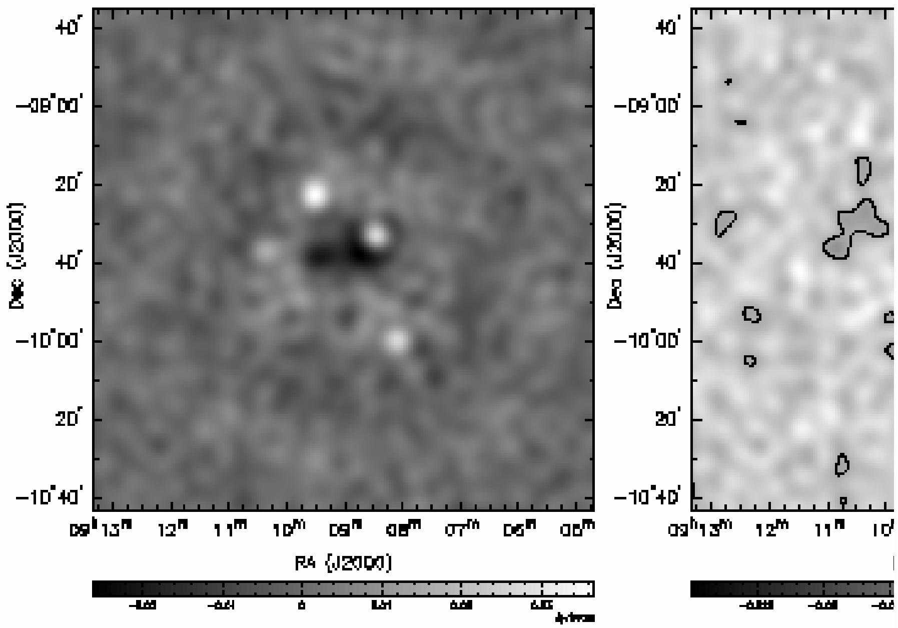

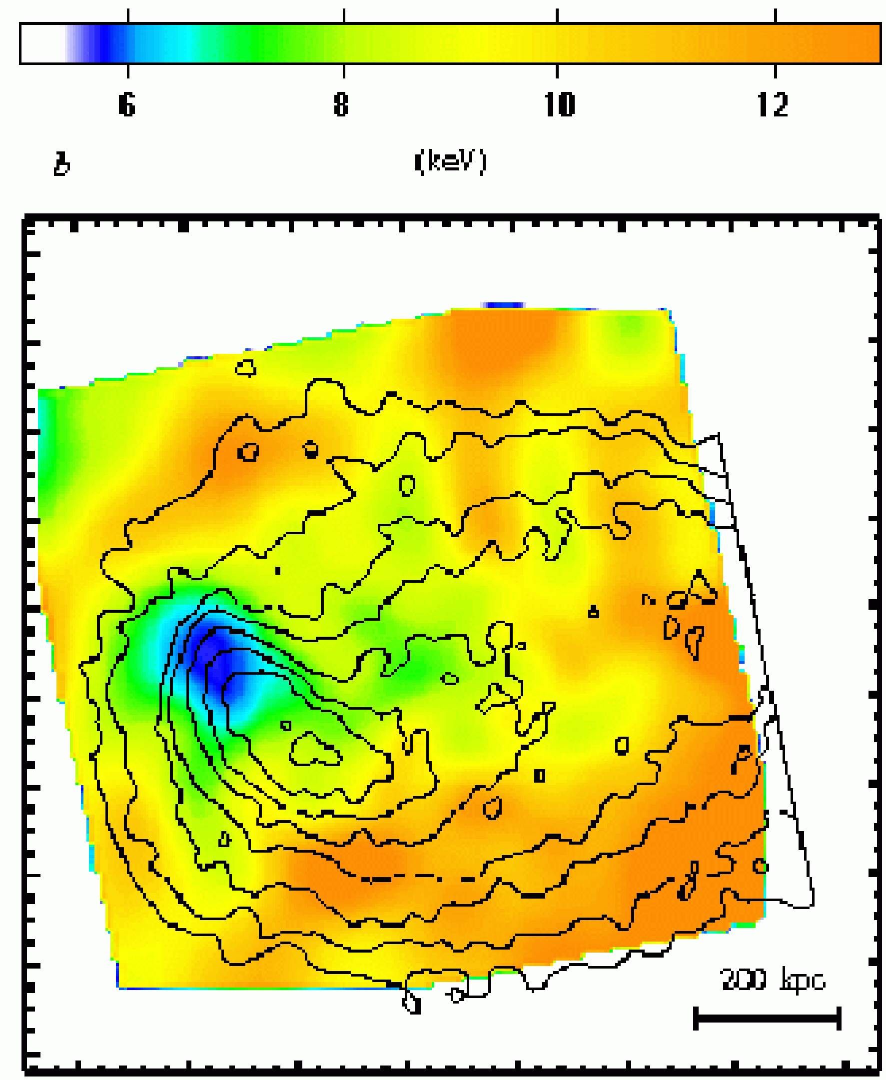

Chandra: Govoni et al. astro-ph/0401421

(left) Raw CBI Image (center) CLEAN so

- A754 – "prototypical" violent m

A1651

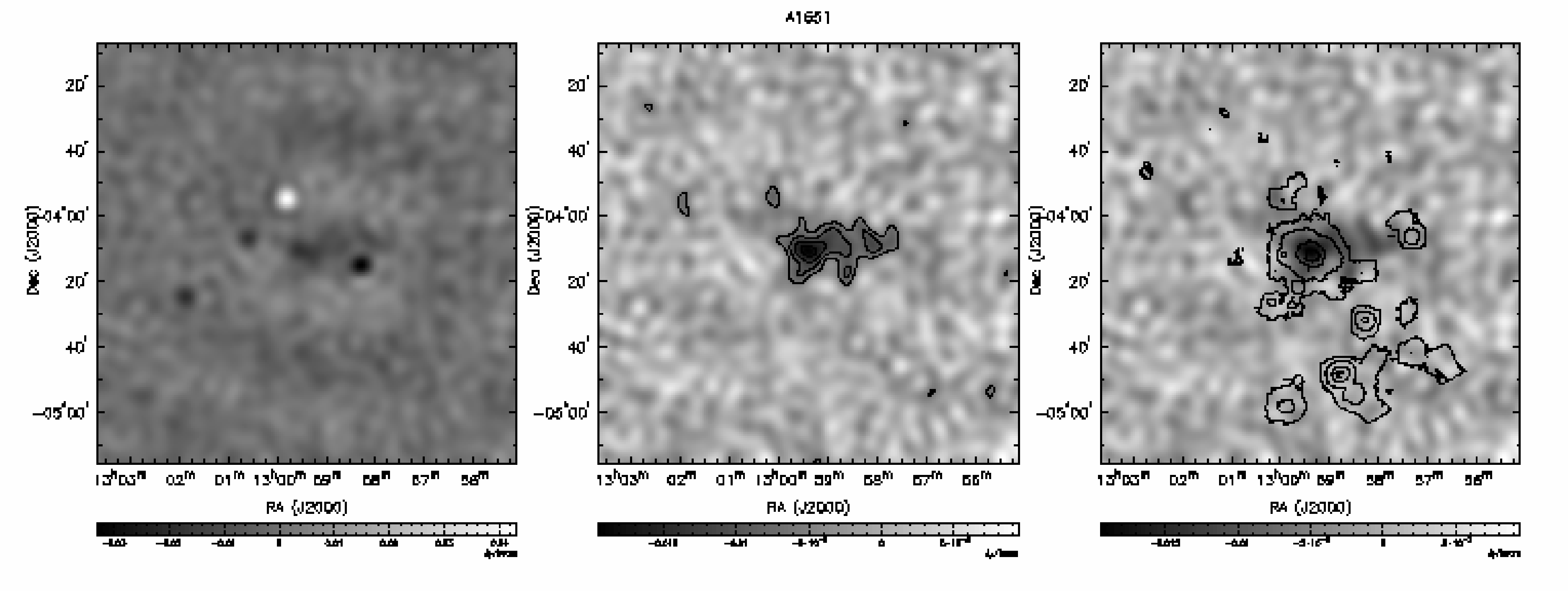

(left) Raw CBI Image (center) CLEAN source-sub CBI Image (right) CBI w/ROSAT

- A1651 – dynamically relaxed cD cluster, unremarkable

A2597

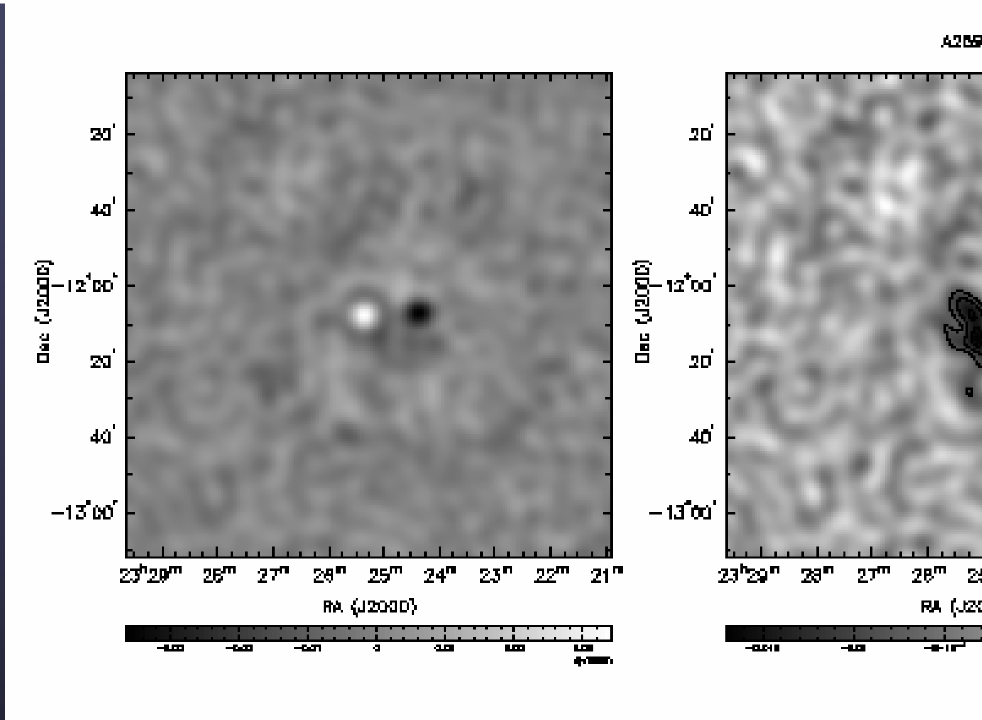

(left) Raw CBI Image (center) CLEAN sourc

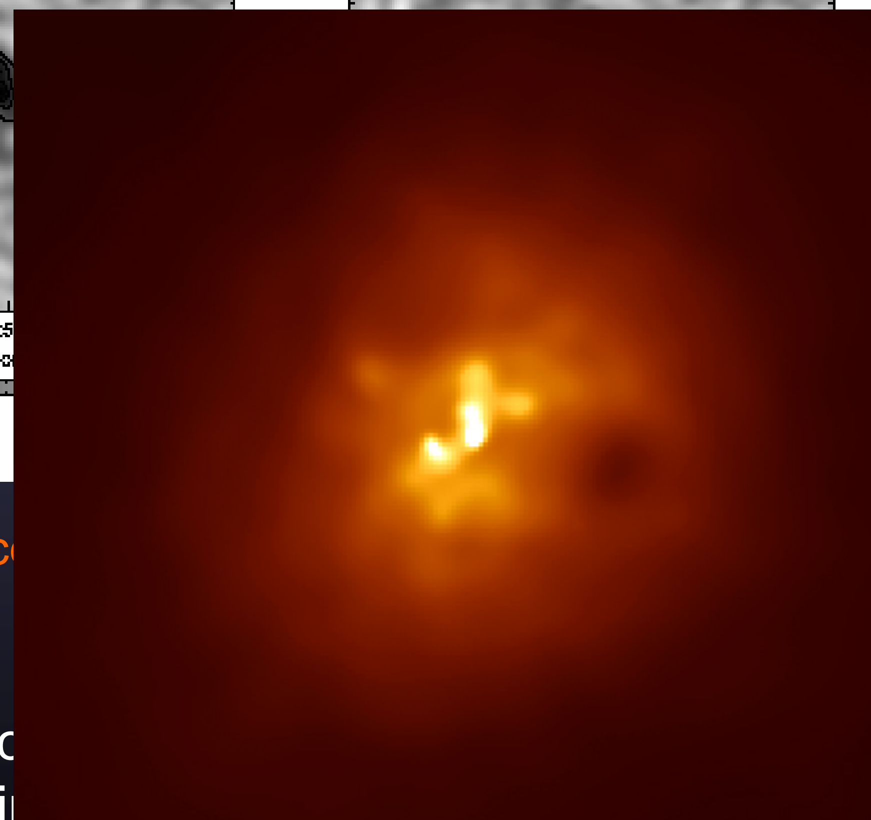

A2597 Chandra, courtesy NASA/CXC/Ohio U/B.McNamara et al.

- A2597 – regular cD cluster with c
  raw image) with X-ray shadows i

Results

- unweighted $H_0 = 67\,^{+30}_{-18}\,^{+13}_{-6}$ km/s/Mpc
- weighted $H_0 = 75\,^{+23}_{-16}\,^{+15}_{-7}$ km/s/Mpc
- uncertainties dominated by CMB confusion
- based on older X-ray data… working on new Chandra/XMM data

Cluster	Corrected $h^{-1/2}$ w/ total random error	ΔT_0 μK	Compton-y_0 $(\times 10^{-4})$
A85	1.23±0.40	-580±190	1.13±0.37
A399	0.24±0.42	-80±130	0.15 ±0.26
A401	1.03±0.29	-620±170	1.20 ±0.34
A478	1.76±0.34	-1800±350	3.49±0.68
A754	1.09±0.31	-560±160	1.09±0.31
A1651	1.42±0.47	-520±170	1.00±0.33
A2597	1.74±1.10	-750±670	1.43±1.28
mean ± sd =	1.22±0.52		
(probability=21%)	$\frac{\chi^2}{\nu}$ = 1.47 for 6 dof		
unweighted sample average: $h^{-1/2}$ =	1.22±0.20		
→	$h = 0.67^{+0.30}_{-0.18}$		
weighted sample average: $h^{-1/2}$ =	1.16±0.14		
→	$h = 0.75^{+0.23}_{-0.16}$		

Error Budget

- CMB anisotropies – the dominant uncertainty
- density model – β models, some bias correction needed
- temperature profiles – assume isothermal, investigate deviations
- radio point sources – residuals small after using counts
- cluster asphericity – < 4%, could be worse in individual clusters
- clumpy gas distribution – $<n_e^2> / <n_e>^2$ bias, substructure?
- peculiar velocities – no bias, 0.04% for even 1000 km/s!
- non-thermal Comptonization – unknown, model dependent

Cluster	CMB error	X-ray mod bias	pt src bias	T_e error	$V_{\rm pec}$ error	CMB+Ther+ptso error
A85	±0.36	1.01	+0.00	0.03	0.05	±0.38
A399	±0.42	1.01	+0.02	0.03	0.05	±0.42
A401	±0.27	1.01	+0.03	0.05	0.04	±0.27
A478	±0.25	1.00	+0.00	0.10	0.04	±0.25
A754	±0.26	1.04	+0.02	0.02	0.04	±0.29
A1651	±0.43	1.00	+0.00	0.06	0.06	±0.44
A2597	±1.06	1.00	+0.01	0.09	0.08	±1.07

ACBAR:

• 16-pixel, multi-frequency, 240 mK, millimeter-wave bolometer array.

• Observes from 2m Viper telescope at the South Pole with 4-5′ beams.

• Bands, filters, detectors, and angular resolution similar to *Planck* HFI.

- Assembled: Fall 2000
- Installed: January 2001
- Upgraded: December 2001
- Observed through Nov 2002

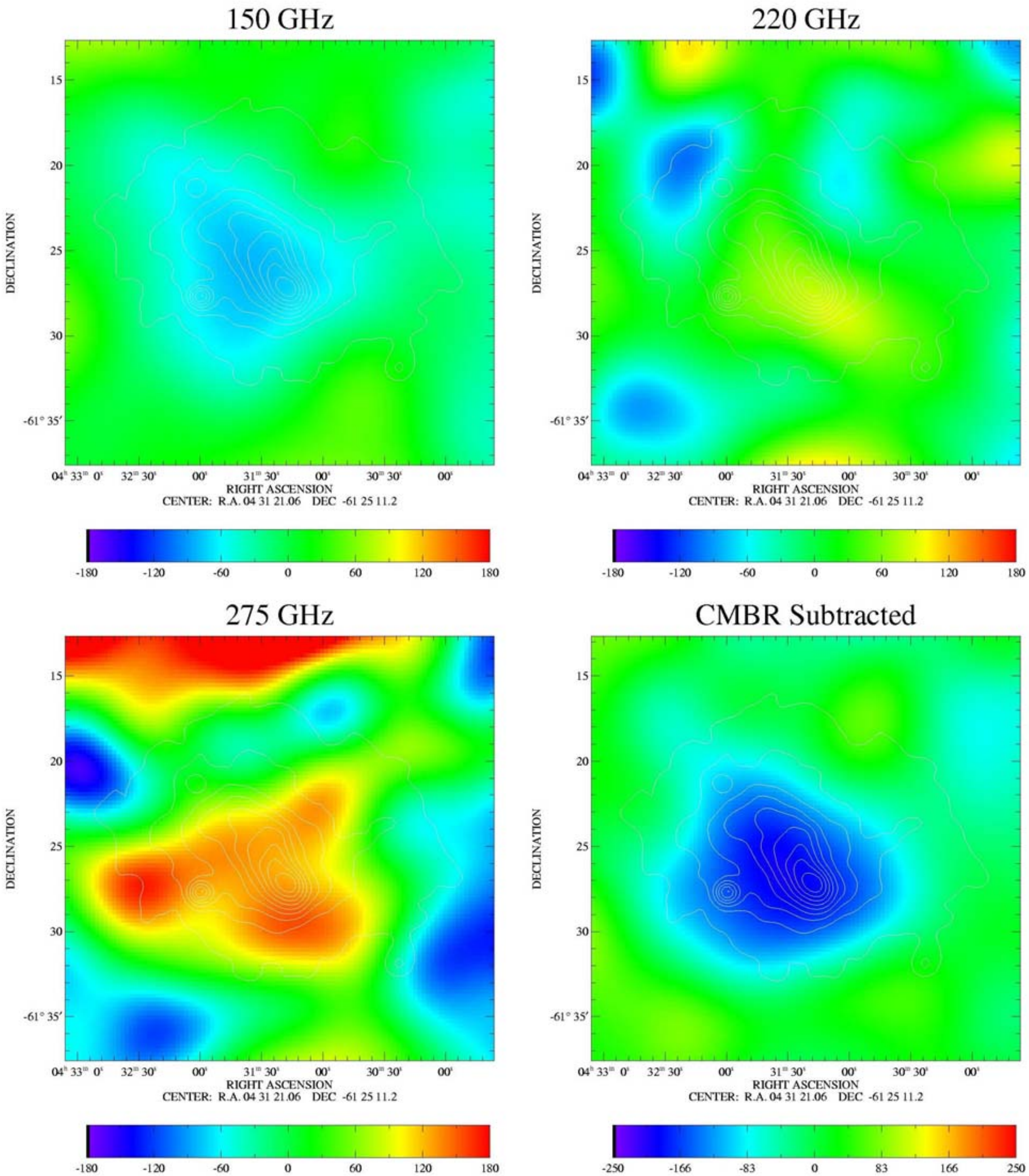

First ACBAR Cluster Image: A3266

z=.0545

T_x=6.2 keV

L_x=9.5x10^{44}

Requires Multi-frequency Data to Subtract CMB

SUZIE

- The Sunyaev-Zel'dovich Infrared Experiment
  - PI: Sarah Church (Stanford)
- Spectrum of the SZE
  - 150, 220, 350 GHz

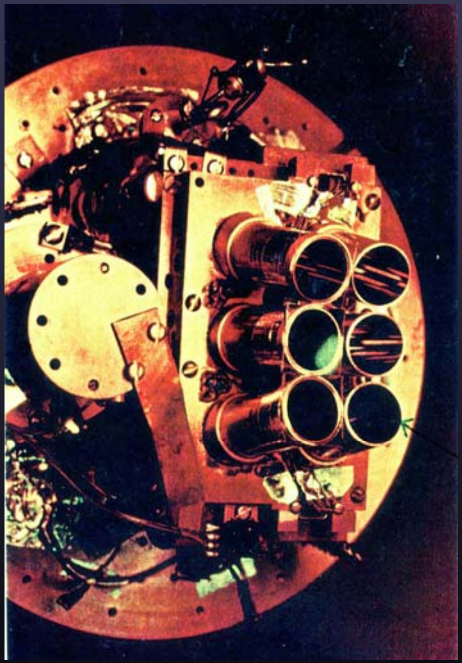

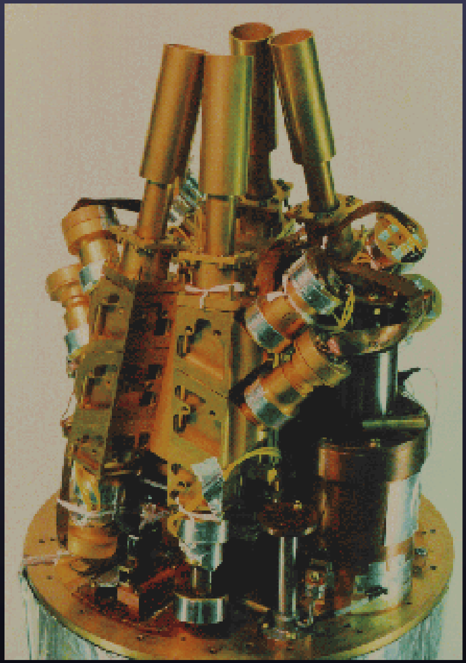

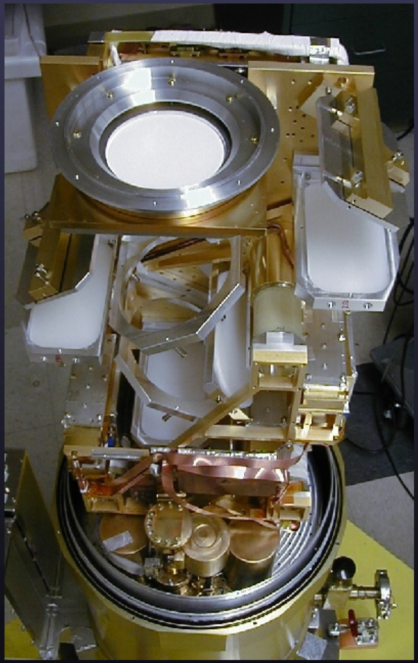

Courtesy SUZIE collaboration: from left - SUZIE I (1991-94), SUZIE II (1994-2003), SUZIE III, CSO on Mauna Kea

SUZIE Science

- SZE spectrum determined by:
  - temperature of cluster gas (tSZ)
  - velocity of cluster (kSZ)

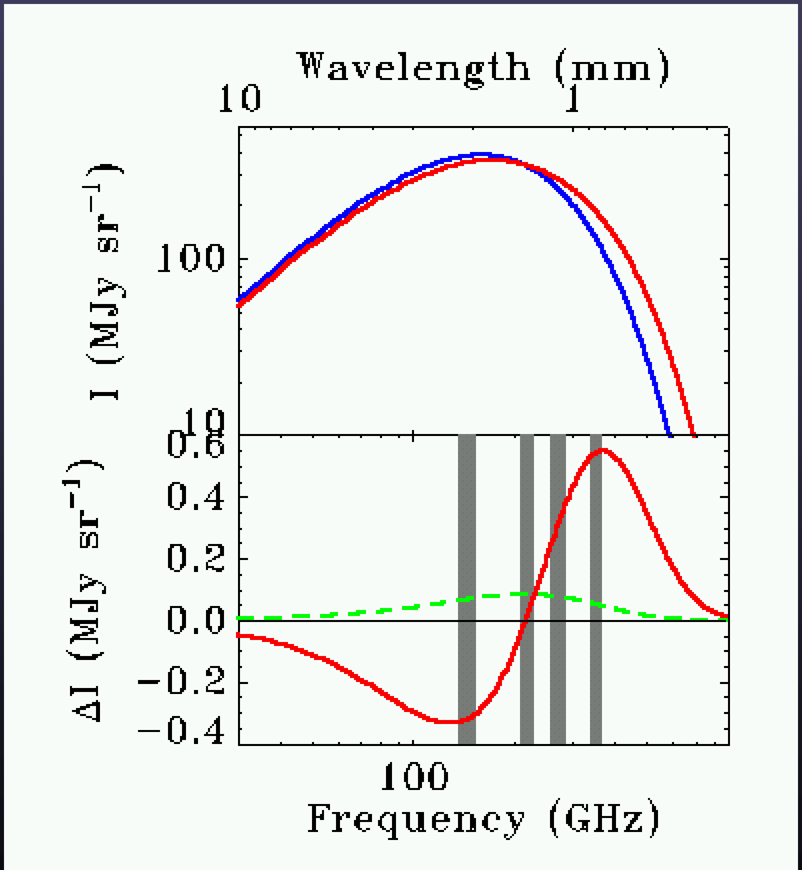

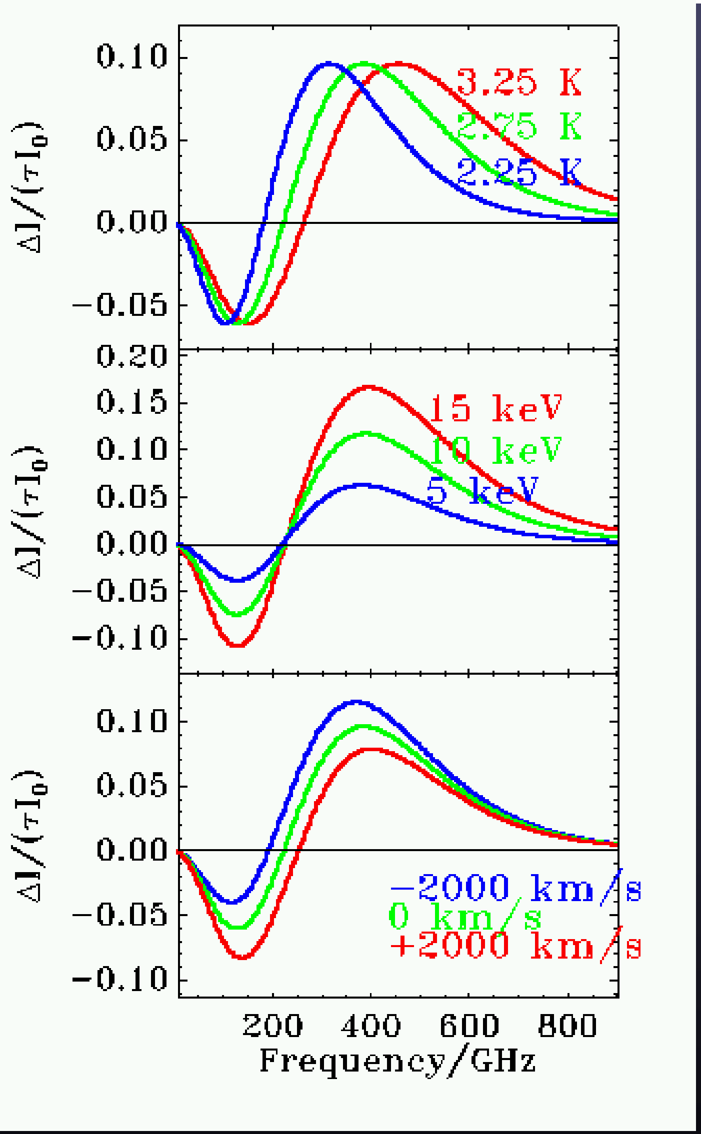

Courtesy SUZIE collaboration

SUZIE Results - spectra

- The SZ spectrum of 11 clusters, as measured by SuZIE II. For each cluster, the solid black line is the best-fit S-Z spectrum, the dashed red line is the best-fit thermal spectrum, and the dotted blue line is the best-fit kinematic spectrum.

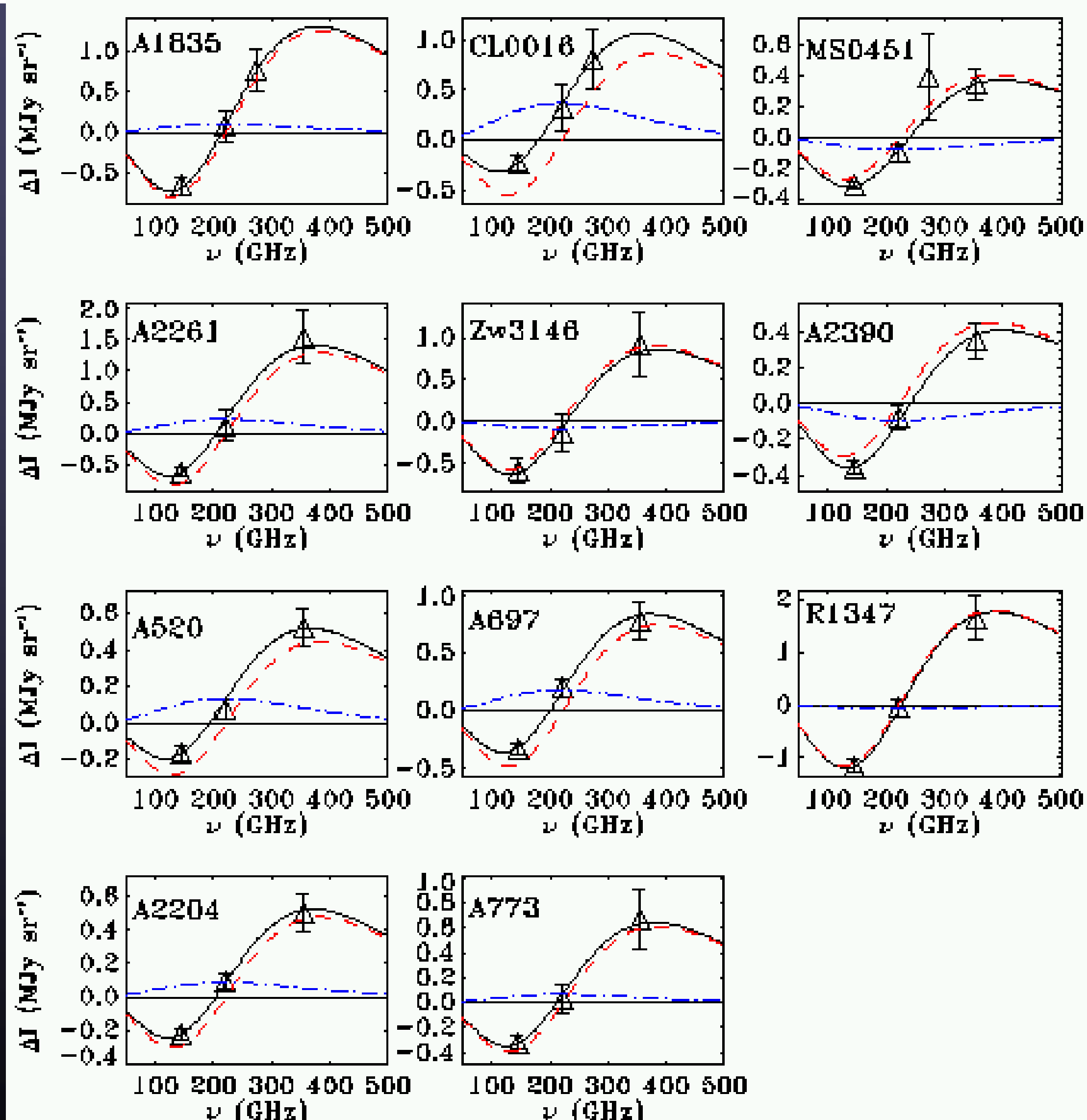

Courtesy SUZIE collaboration

SUZIE Results - velocities

- Measurements of each cluster's peculiar velocity plotted against redshift. The cross-hatched region shows the range that has been probed using optical measurements of peculiar velocities.
- Included are previous peculiar velocity measurements of the clusters A1689 and A2163 observed with the SuZIE I receiver by Holzapfel et al. (1997).

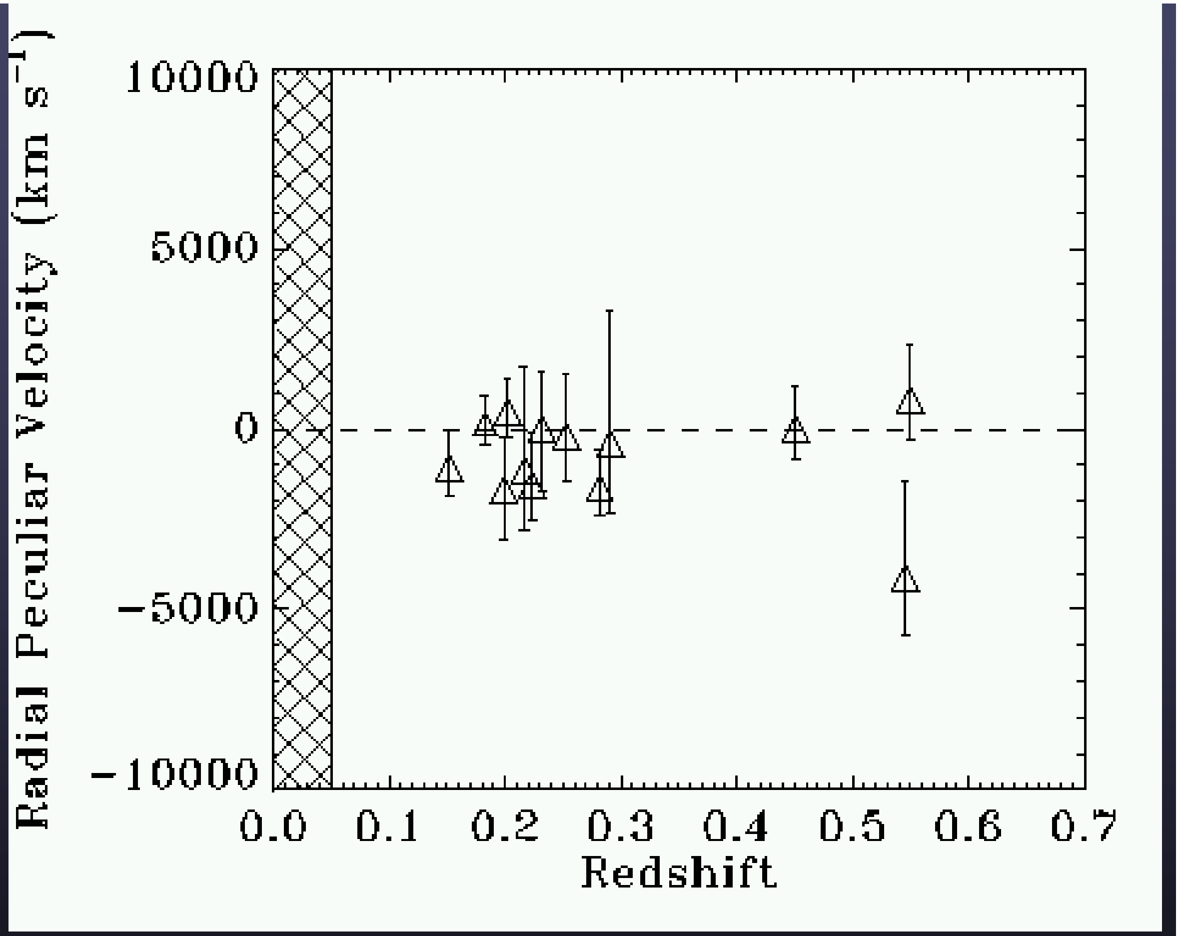

Courtesy SUZIE collaboration

Future SZ

- The Sunyaev-Zeldovich Array (SZA)
  - 8 antennas, 3.5m diameter, 30 GHz
  - 6 x 10.4m OVRO
  - 11 x 6m BIMA
  - Combined array
  - CARMA site in Owens Valley - CA
- Big Bolometer Arrays (APEX and SPT)
  - APEX (MPI) at ALMA site, Chile
  - South Pole Telescope (Chicago)
  - 1000+ element bolometer cameras 150 GHz
  - surveys for SZ clusters
  - constraint growth and volume factors
  - dark energy density Ω_e and equation of state w_e

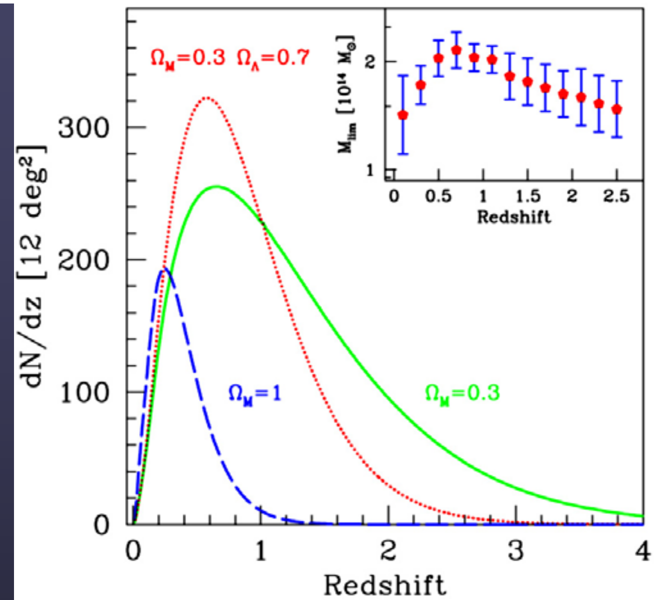

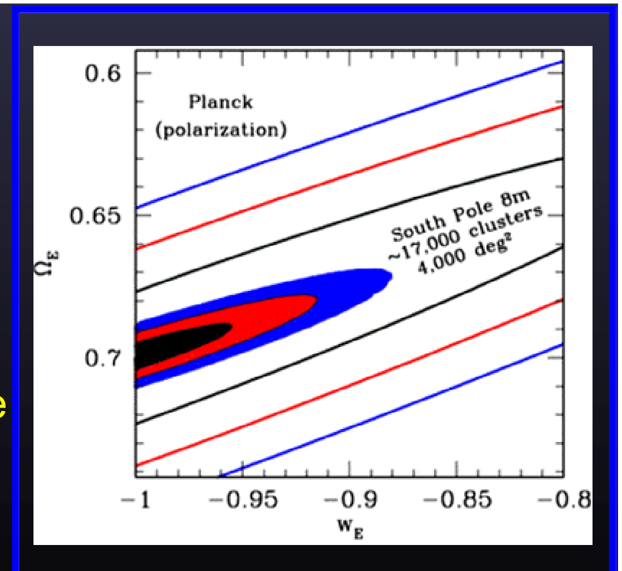

Courtesy SZA and SPT collaborations

Matter Spectrum and Large Scale Structure

After recombination …

- Potential fluctuations grow to form Large Scale Structure
  - overdensities collapse to form galaxies and galaxy clusters
  - underdensities expand into voids, with cosmic web between
  - acoustic peaks appear as Baryon Oscillations in matter spectrum

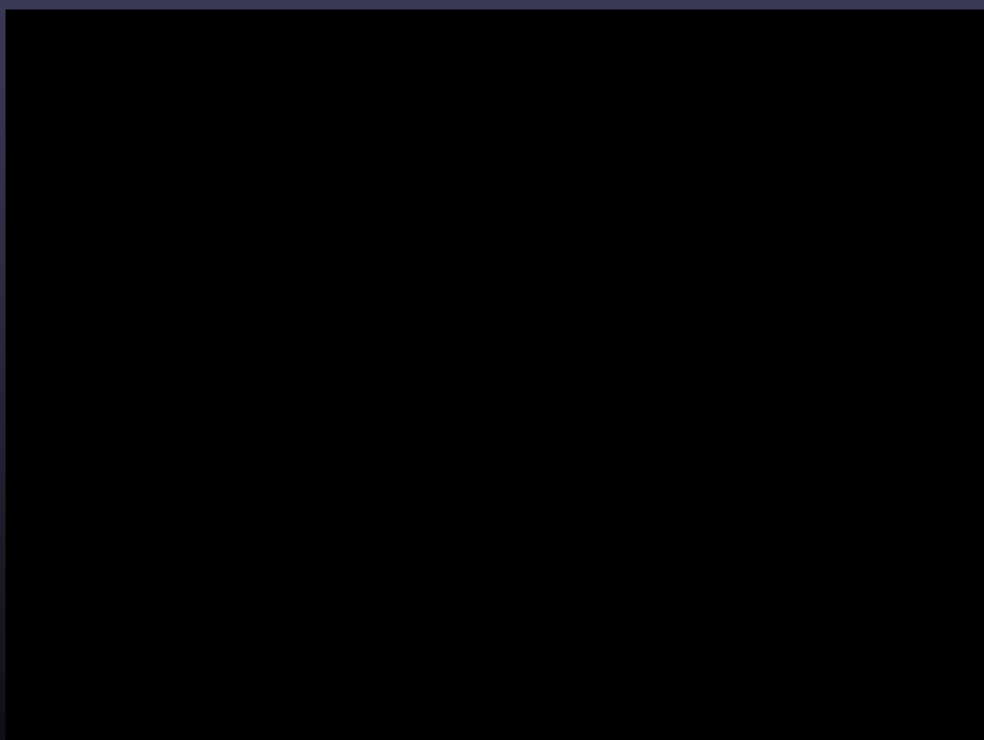

Simulation courtesy A. Kravtsov – *http://cosmicweb.uchicago.edu*

After recombination …

- Potential fluctuations grow to form Large Scale Structure
  - overdensities collapse to form galaxies and galaxy clusters
  - underdensities expand into voids, with cosmic web between
  - acoustic peaks appear as Baryon Oscillations in matter spectrum
- Current overdensities in non-linear regime
  - $\delta\rho/\rho \sim 1$ on 8 h^{-1} Mpc scales (σ_8 parameter)
  - linear potential growth: $\delta\rho/\rho \sim$ 10-3 at recombination ($z \approx 1500$)

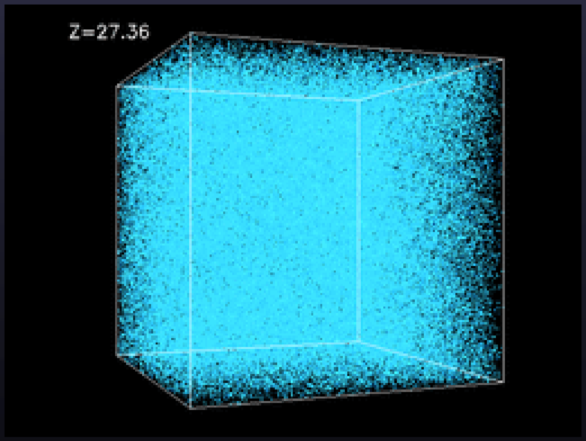

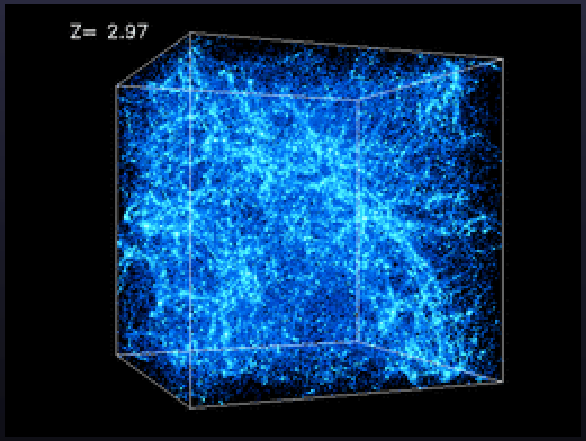

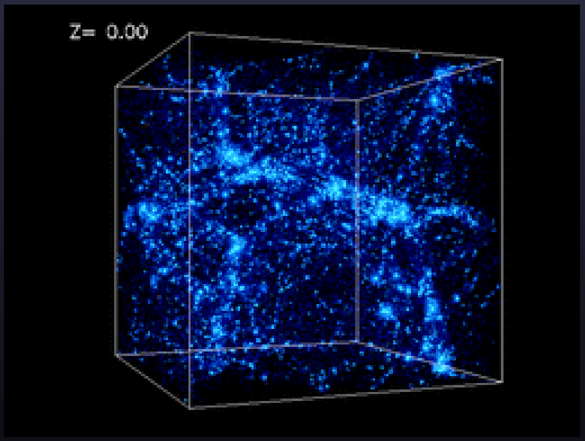

Simulation courtesy A. Kravtsov – *http://cosmicweb.uchicago.edu*

Late Times: Matter Power Spectrum

- matter power spectrum P(k)
  - related to angular power spectrum (via transfer function)

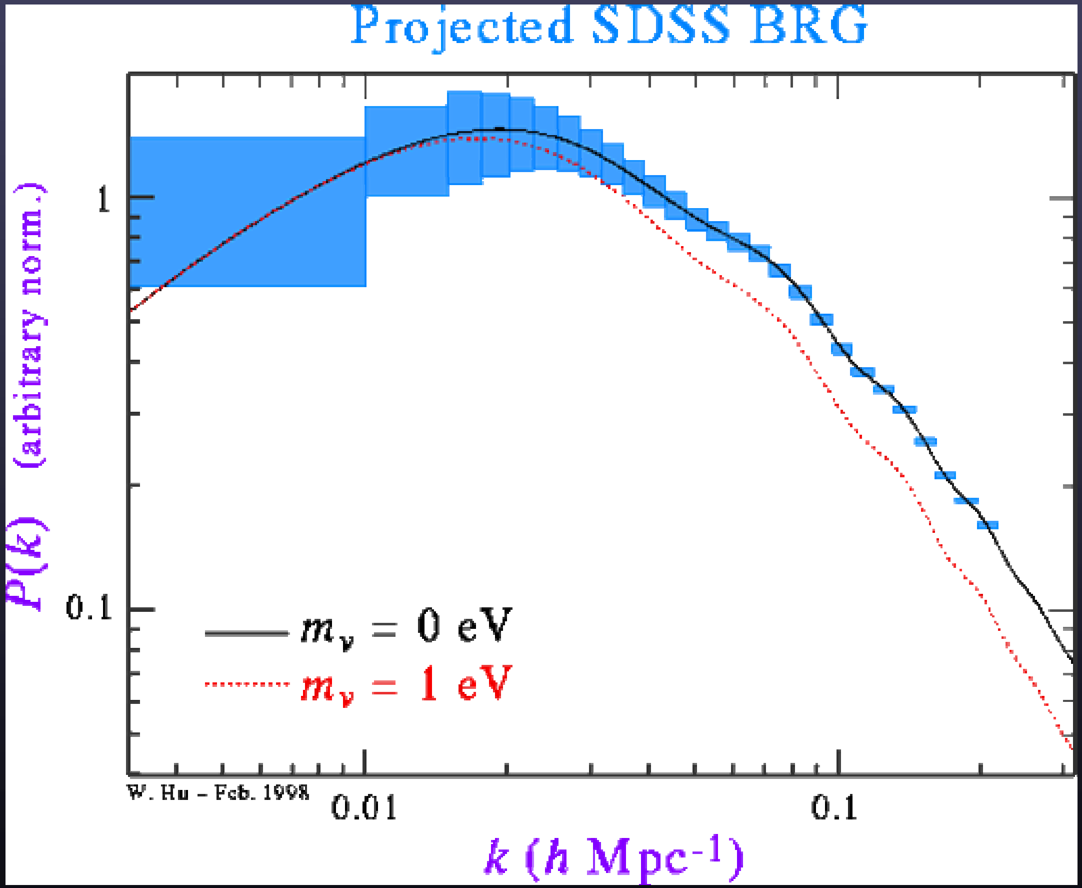

- large scale structure
  - non-linear on small scales (<10 Mpc = 0.1)
  - imprint of CMB acoustic peaks retained on large scales
  - "baryon oscillations" measured by SDSS

Courtesy Wayne Hu – *http://background.uchicago.edu*

Late Times: Matter Power Spectrum

- matter power spectrum P(k)
  - related to angular power spectrum (via transfer function)

- <u>large scale structure</u>
  - non-linear on small scales
  - imprint of CMB acoustic peaks retained on large scales
  - “baryon oscillations” measured by SDSS

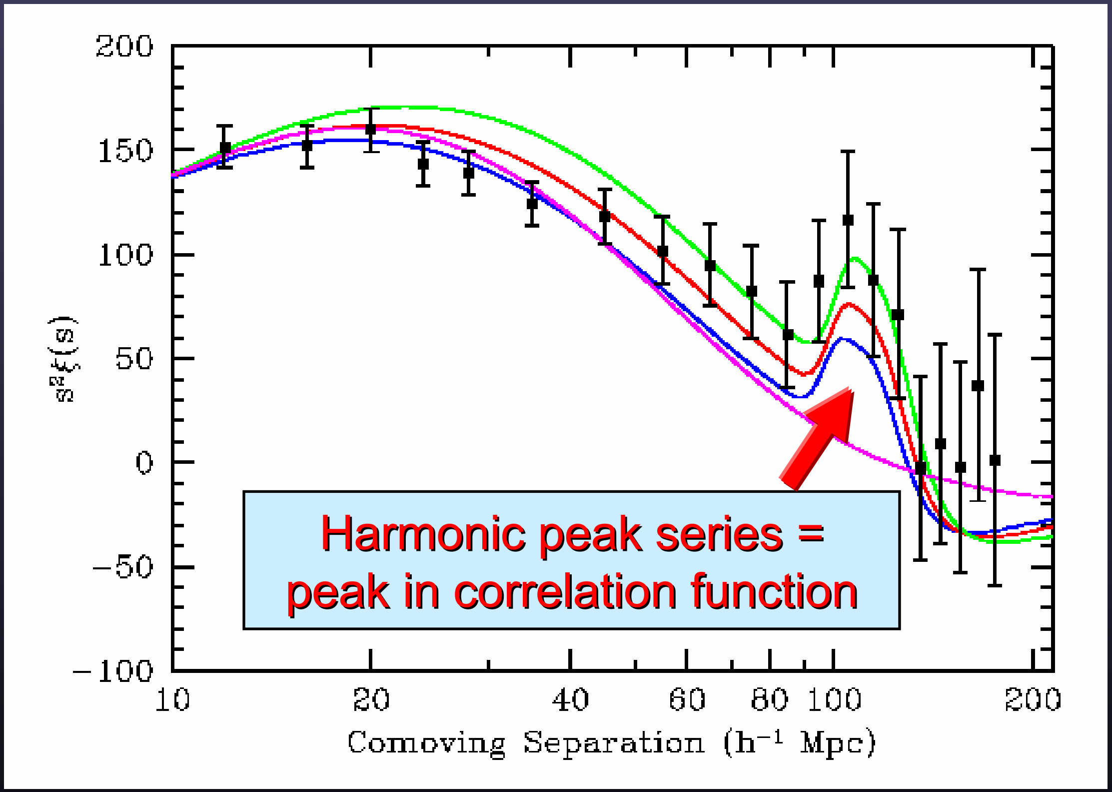

Eisenstein et al. 2005, astro-ph/0501171

Dark Energy, Galaxies, and the Late ISW

Galaxies and ISW

- The distribution of galaxies should reflect the distribution of potential wells in nearby Universe
  - Sloan Digital Sky Survey (SDSS)
- The decay of potential during epoch of Dark Energy domination (z>2) causes the Late ISW in the CMB
  - low-ℓ CMB anisotropies in WMAP
- Cross-correlate WMAP with SDSS

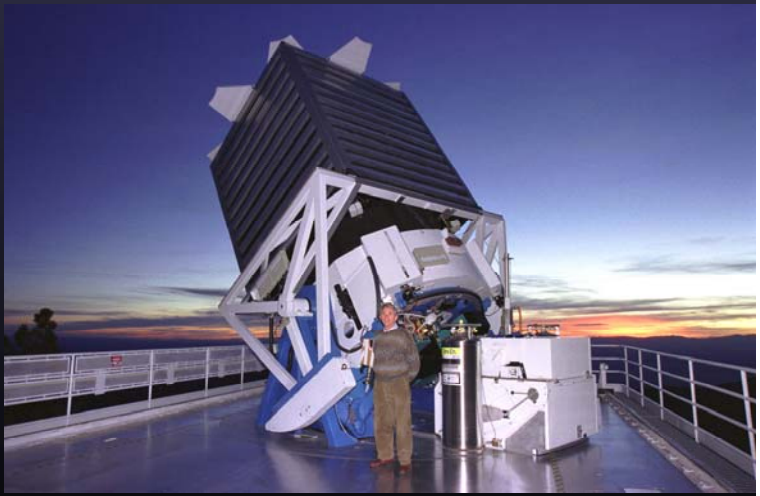

Courtesy SDSS collaboration

WMAP and SDSS

- cross-correlation should enhance ISW signal

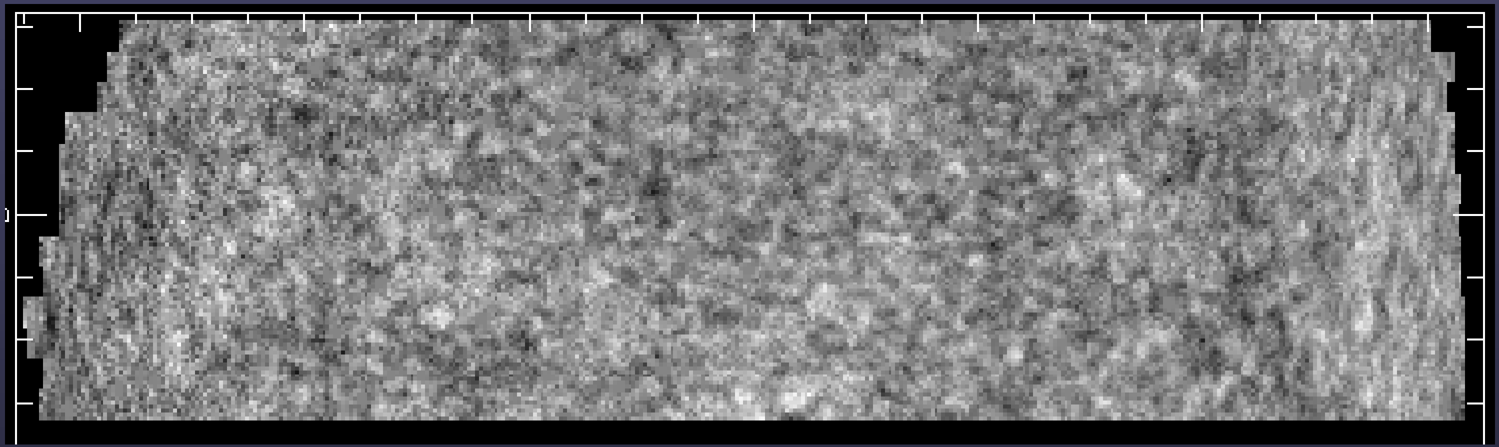

WMAP W band temperatures across 50% of SDSS area

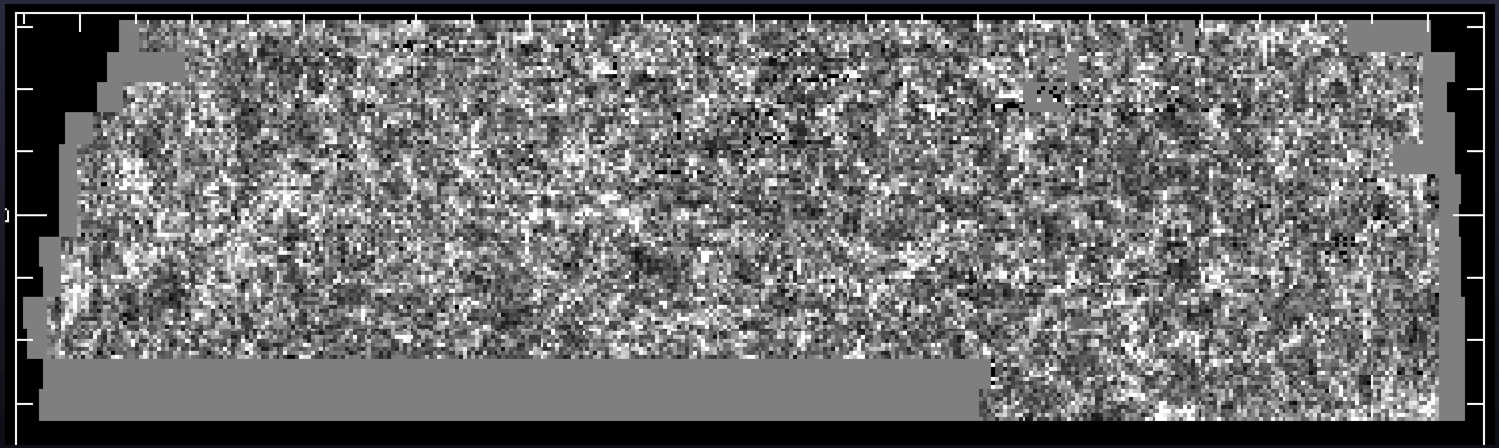

Courtesy Bob Nichol

Density of Luminous Red Galaxies (LRGs) selected from the SDSS

SDSS-WMAP correlation results

- LRG selection to z~0.8 (Eisenstein et al. 2001)
- 5300 sq degrees
- Achromatic (no contamination)
- Errors from 5000 CMB skies
- Compared to a null result
- >95% for all samples
- Low redshift sample contaminated by stars
- Individually >2s per redshift slice
- 4 redshift shells (not significant overlap)

- <u>Overall, signal detected at ~5σ</u>

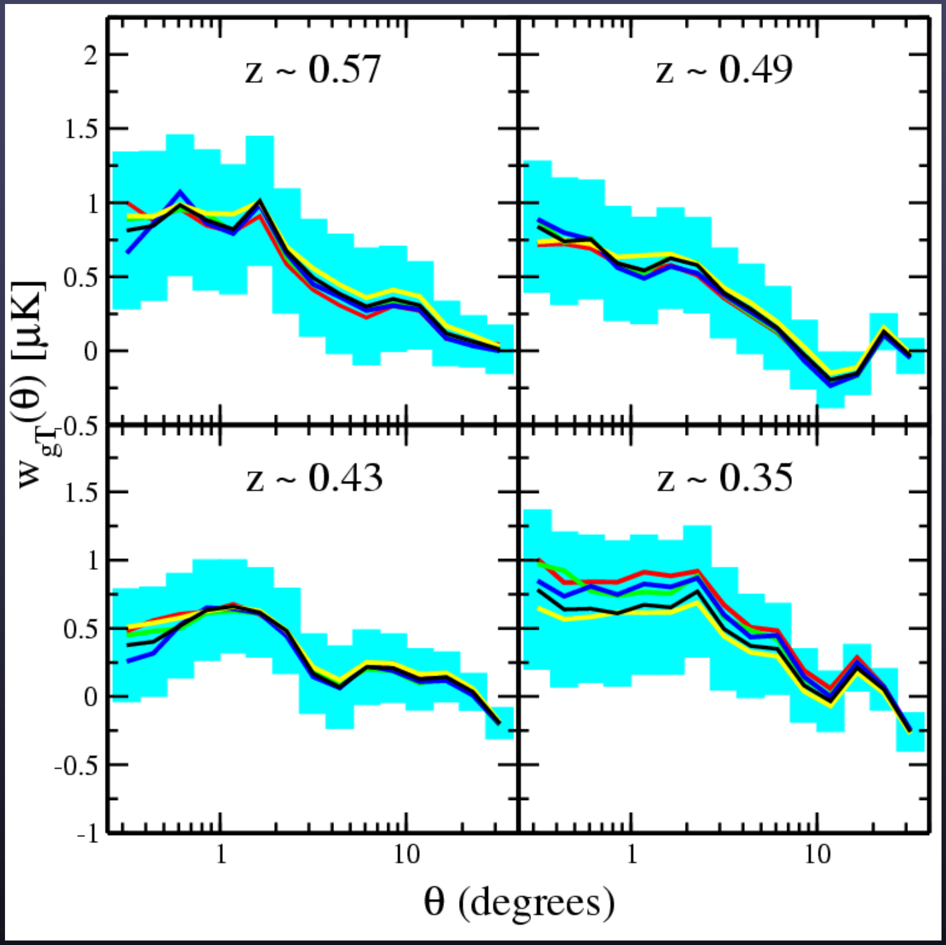

Courtesy Bob Nichol for SDSS team

ISW predictions

- Halo model. Biasing of b=1,2,3 & 4 for LRGs
- Plus SZ on small scales
- Data prefers DE model over null hypothesis at the >99% confidence for all combinations
- The measurement is very sensitive to n(z) assumed and Ω_m

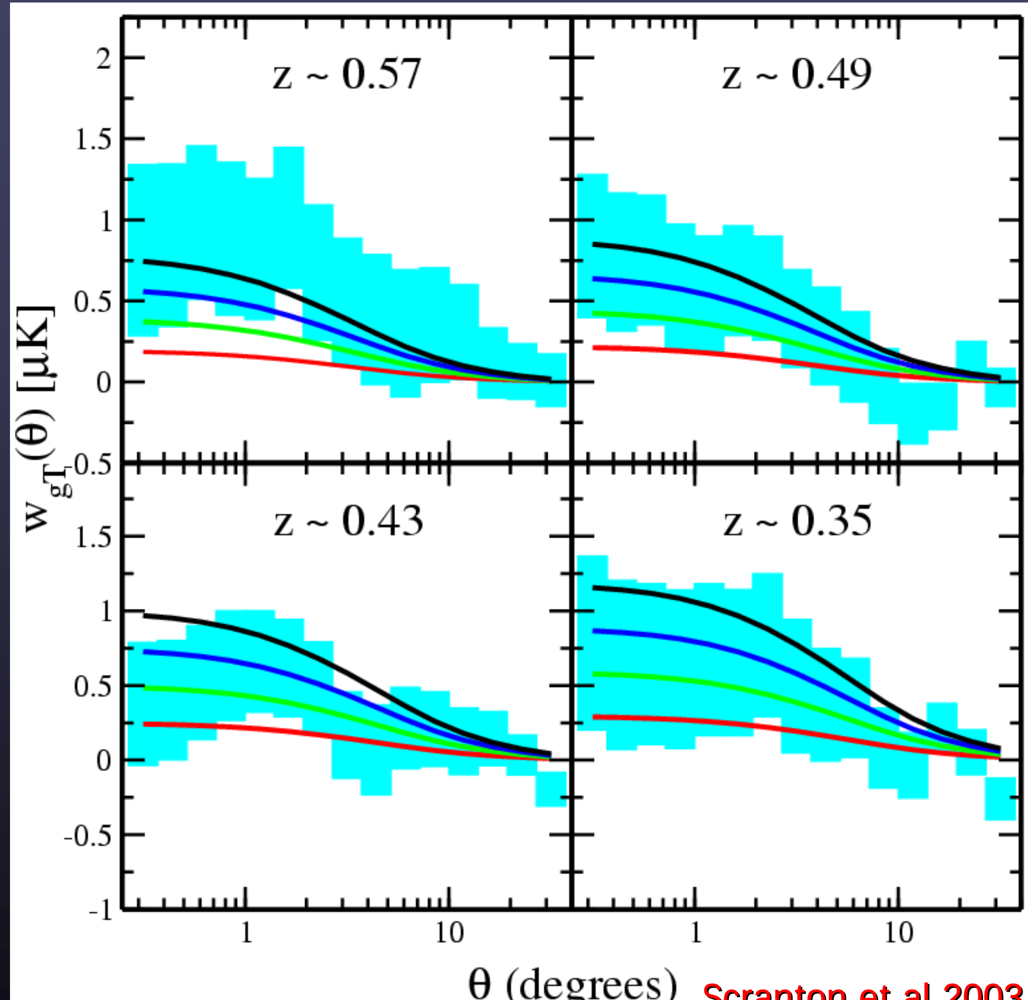

Scranton et al 2003

Courtesy Bob Nichol for SDSS team

Summary

CMB Checklist (finale)

Structure predictions from inflation-inspired models:

- late-time non-linear structure formation (revisited)
  - gravitational lensing of CMB
  - √ Sunyaev-Zeldovich effect from deep potential wells (clusters)
- growth of matter power spectrum
  - √ primordial power-law above current sound horizon
  - √ CMB acoustic peaks as baryon oscillations
- dark energy domination at late times
  - √ correlation of galaxies with Late ISW in CMB
  - cluster counts (SZ) reflect LCDM growth and volume factors

It does look like our current Universe is dominated in energy density by a Dark Energy (Lambda) component!